Jordan Journal of Civil Engineering, Volume **18**, No. **4**, **2024**
DOI: https://doi.org/10.14525/JJCE.v18i4.02

Jordan Journal of Civil Engineering

Journal homepage: https://jjce.just.edu.jo

Study on the Stress and Deformation Laws and Work Principles of the Pull-pile Supporting Structure in a Deep Foundation Pit

Binpeng Lan [1], Yanping Wang [1]*, Weiguo Wang [1], Yijun Wang [2], Ke Ruan [3]

[1] *School of Civil Engineering and Geomatics, Shandong University of Technology, Zibo Shandong 255049, China.*
[2] *Chengdu Institute of Survey and Investigation, Chengdu Sichuan 610084, China. * Corresponding Author.*
[3] *Tianjinchengjian University, School of Materials Science and Engineering, Tianjin 300384, China.*

ARTICLE INFO

Article History:
Received: 8/3/2024
Accepted: 13/7/2024

ABSTRACT

In combination with the field monitoring data, PLAXIS3D finite-element software was used to numerically model the pull-pile supporting structure in a deep foundation pit. This structure was compared to the single-row pile support structure in order to learn more about the pull-pile supporting structure's force and deformation characteristics and how it works. The study found that the cumulative horizontal displacement curves of the supporting piles are integrated into an “upward convex” shape. The bending-moment curve of the front-row piles presents an “inverted S” shape, and the bending-moment curve of the back-pull piles presents a “bow” shape. The “back-pull-pile effect” can improve the unbalanced distribution of positive and negative bending moments in single-row piles by changing the stress condition of the soil. In other words, the pull-pile supporting structure has good safety and serviceability and can well control the lateral displacement of the foundation pit.

Keywords: Deep foundation pit, Pull-pile supporting structure, Stress and deformation laws, Work principles.

INTRODUCTION

The pull-pile supporting structure (PPSS) is mostly used in deep foundation pit wall-protection engineering, which is a temporary, gravity-driven, and rigid wall-protection enclosure structure to ensure the smooth construction of the underground part of the main structure and the safety of the surrounding environment of the foundation pit (Ye et al., 2020; Zhou et al., 2021). With the vigorous development of urbanization, the number of underground space projects is increasing, and the surrounding environment faced by deep foundation pit projects is also becoming more and more complicated (Sun et al., 2012; Zhou et al., 2022). Due to its features, which include a small number of supporting piles, convenient construction, a small footprint, and excellent anti-lateral displacement performance, the PPSS has attracted significant attention despite the influence of the dense infrastructure of the intricate environment and the meager funding (Yu et al.,2019; Zhang et al.,2020). The PPSS is a spatially integrated support structure formed by adding certain arrangement rules and a number of back-pull piles to the rear of the existing single-row piles and connecting the front-piles and pull-piles through connecting beams (Mo et al., 2022; Yang et al.,2023), as shown in Figure (1).

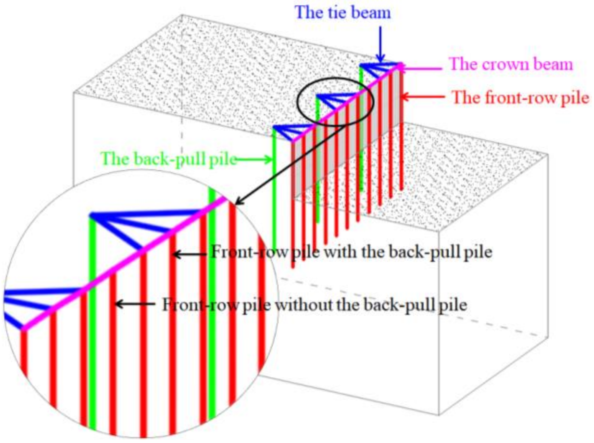

Figure (1): The pull-pile support structure schematic diagram

The associated research about the supporting structure for deep foundation pits has produced successful outcomes in recent years. Qian et al. (2011), Gu (2014), Zhou et al. (2016), and Yang et al. (2020) studied the deformation characteristics of traditional double-row pile support structures and the differences in displacement and internal force between front piles and back piles and further analyzed the reasons for the differences. Wang et al. (2024) conducted a comparative analysis of the mechanical differences between the double-row pile support structure and the single-row pile support structure, which can provide an important enlightenment for similar projects. Jiang et al. (2022), Gan et al. (2023), Guo et al. (2023), and Liu et al. (2022) studied the deformation-evolution characteristics, working behavior, and the influence of row spacing and pile spacing on the supporting performance of a vertical-incline (incline - vertical) double-row pile supporting structure. Zhu et al. (2024) carried out finite-element analysis on the stepped three-row pile supporting structure and successfully verified its stability based on actual projects. Zhou et al. (2021) proposed for the first time a double-row pile support structure with strong pre-stressed constraints and conducted a comparative analysis with the traditional double-row pile support structure. The results showed that the new double-row pile support structure has smaller deformation and lower cost. However, there are few studies on the PPSS with relevant data. So, this study will use the PPSS in a foundation pit supporting project in Chengdu as its research background. It will then analyze the supporting effects of the PPSS and the single-row pile supporting systems to learn more about the PPSS's stress deformation laws and how it works.

ENGINEERING BACKGROUND

Overview of the Project

Dongshan apartment project is located in Chengdu, China (N: 30.52738913, E: 104.24334526). It is surrounded by municipal roads and residential projects under construction and with completed construction. The project consists of a two-story basement. The safety level of the foundation pit is with an importance coefficient of $\gamma = 1.1$. The section AB protected by the PPSS of the foundation pit is an example. The excavation depth is 8.5 m; the diameter of the piles is 1.2 m; the pile spacing is 2.0 m; the pile length is 17.5 m (including the crown beam, the width of which is 1.2 m and the thickness is 1.0 m); and the length of the embedded end is 10.0 m. The layout of the foundation pit is shown in Figure (2).

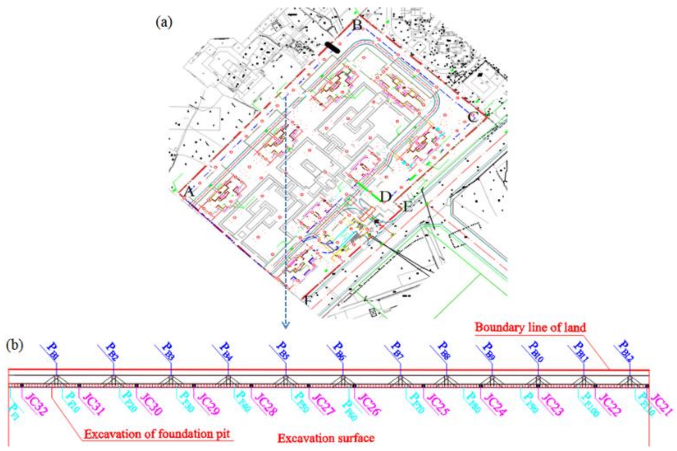

Figure (2): Layout of the foundation pit

Engineering Geological Survey

After on-site investigation, the distribution profile of the borehole soil layer of the apartment project is shown in Figure (3). After the investigation, the buried depth of pore water stable water level was -9.9 ~-12.1m. The dewatering of the foundation pit is controlled near -25m. The soil parameters obtained based on geotechnical tests are reduced to 0.8 times due to the expansion of the soil and the disturbance of the soil sample during the parameter-acquisition process. The parameters of each soil layer after reduction are shown in Table 2. Miscellaneous fill: composed of rock blocks, construction slag, abandoned slag fragments, cohesive soil, …etc., the structure is messy, loose, and underconsolidated. Cohesive soil is mainly hard plastic, slow dip cracks developed, and gaps were filled with grayish white clay minerals. Silty clay is mainly malleable medium dense silt, and mica flakes can be seen. Pebble-containing silty clay is medium dense, mainly composed of pebbles, mixed with a small amount of drift stone. Fully weathered shaly sand is mainly plastic, partially crushed rock, and hands can be pinched.

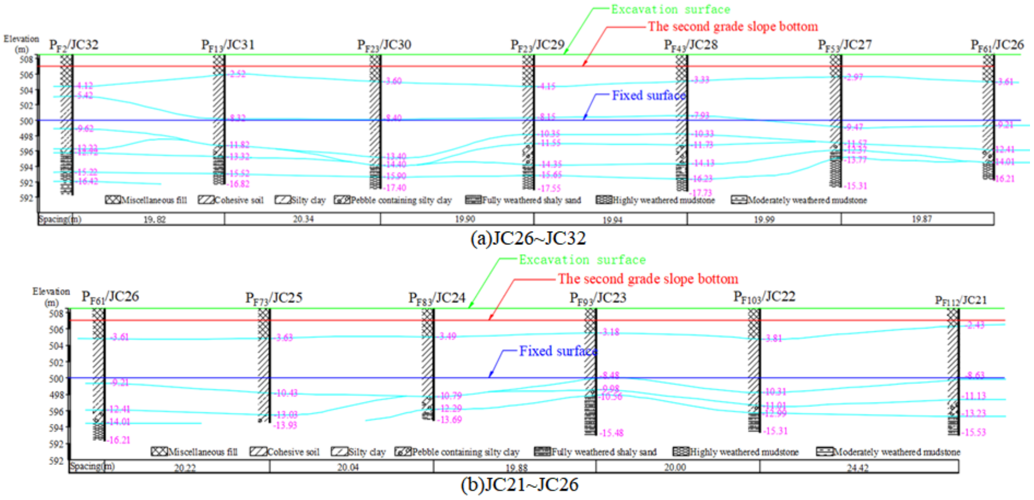

Figure (3): Distribution profile of the borehole soil layer

Table 1. Simulated construction conditions

Soil layer	**γ (kN/m^3)**	***c* (kN/m^2)**	**φ (°)**	**E_{50}^{ref} (kN/m^2)**	**E_{oed}^{ref} (kN/m^2)**	**E_{ur}^{ref} (kN/m^2)**	**G_0^{ref} (kN/m^2)**
Miscellaneous fill	18.0	8.0	16.0	$4e^3$	$4e^3$	$20e^3$	505^3
Cohesive soil	19.0	48.0	24.0	$7e^3$	$7e^3$	$28e^3$	$90e^3$
Silty clay	18.5	28.8	19.2	$6e^3$	$6e^3$	$24e^3$	$66e^3$
Silt	18.0	9.6	32.0	$4.5e^3$	$4.5e^3$	$12e^3$	$70e^3$
Pebble-containing silty clay	20.5	16.0	28.8	$12e^3$	$12e^3$	$36e^3$	$150e^3$
Fully weathered shaly sand	19.5	44.8	32.0	$7e^3$	$7e^3$	$21e^3$	$90e^3$
Highly weathered mudstone	19.5	50.0	25.0	$84e^3$	$84e^3$	$250e^3$	$1050e^3$
Moderately weathered mudstone	22.5	140.0	50.0	$100e^3$	$100e^3$	$300e^3$	$1250e^3$

Note: In the table, γ is the natural bulk density of soil. E_{50}^{ref} is the secant stiffness of the standard triaxial drainage test; E_{oed}^{ref} is the tangent stiffness of the confined compression test; E_{ur}^{ref} is the unloading/reloading stiffness; and G_0^{ref} is the small strain reference shear modulus.

Testing Schemes

There are 12 back-pull piles (P_{B1}~P_{B12}) and 112 front piles in the pull-pile supporting section (P_{F1}~P_{F112}) in this foundation pit project. As seen in Figure 2(b), the 12 monitoring locations (JC21~JC32) are situated near the front piles.

Field Monitoring Program

The hardening-soil model with small-strain stiffness (HSS) in PLAXIS3D finite-element analysis software considers the strain dependence of soil load history and stiffness and can simulate the different responses of soil in the range of small strain to large strain. HSS can take into account that the plastic part of the deformed soil is not recoverable during unloading, which plays a crucial role in accurate engineering simulations and calculations. Therefore, PLAXIS3D finite-element analysis software was chosen for numerical modeling, with the following assumptions.

Based on engineering practice and combined with engineering experience, the elastic modulus of the front-row pile, the back-pull pile, the crown beam, and the connecting beam all using C30 reinforced concrete is 3.2 GPa, and the elastic modulus of the concrete slab is 2 GPa. The information about the borehole soil layer at the location of each monitoring point is shown in Figure (4). Considering the driving load on the top of the foundation pit slope and the construction of the pit bottom structure, according to the most dangerous situation design, 30 kPa is applied at a distance of 5 m from the top of the foundation pit slope, and a 185 kPa long-term load is applied to the bottom of the pit after the excavation of the foundation pit. Soil-layer distribution refers to the soil-layer information of the borehole in Figure (3), and for soil parameters, refer to Table 1. The dimension parameters of PPSS are consistent with the actual project.

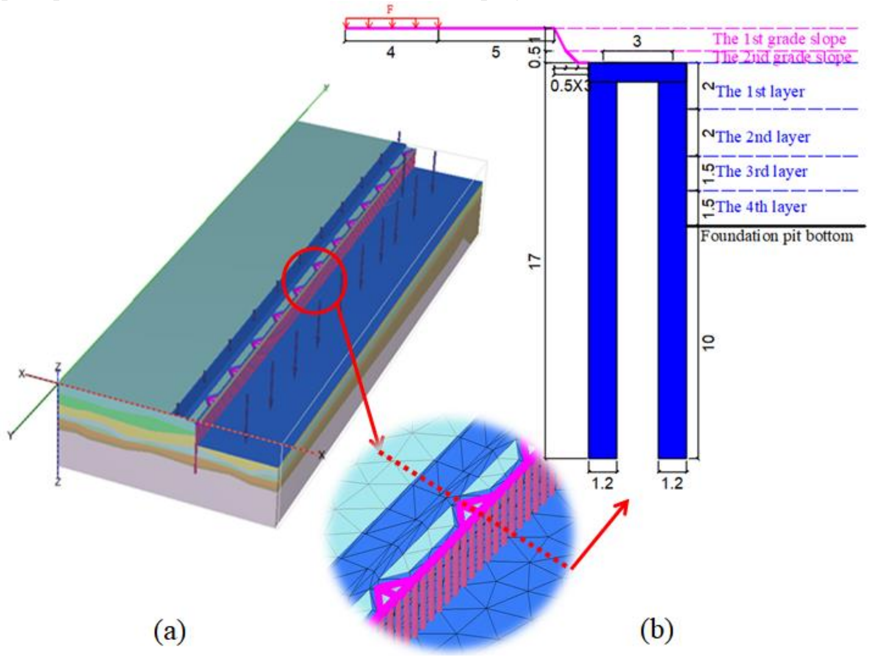

Figure (4): Modeling diagram of the PPSS

Analysis of Test Results

Analysis of Field Monitoring Results

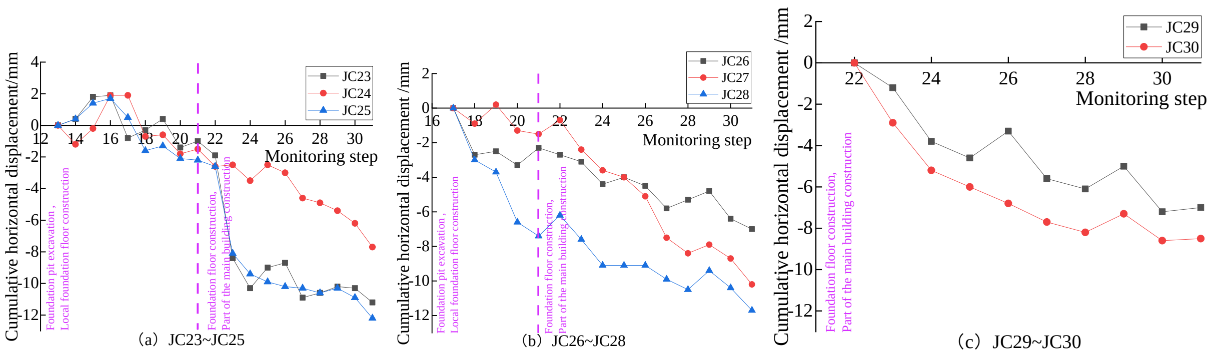

Figure (5): The cumulative horizontal displacement curve of monitoring points

As can be seen from Figure (5), the cumulative horizontal displacement of each monitoring point shows an overall increasing trend; that is, with the increase in monitoring steps, the cumulative horizontal displacement of piles in front of each monitoring point increases on the whole. The cumulative horizontal displacement curve of each monitoring point has a "W"-shaped fluctuation trend in a short period of time, which is manifested in the different amplitude rise of the horizontal displacement curve of the front-row pile. Because the construction of the supporting piles is a jumping pile, the subsequent supporting pile will have an instantaneous impact on the surrounding soil during the concrete-pouring process. The extrusion and instantaneous effects will be sent to the existing supporting piles through the soil between the piles. This will cause the existing supporting piles to move horizontally with amplitudes that vary.

After the pouring of the supporting piles at the monitoring points JC23 ~ JC25 is completed, the horizontal lateral displacement monitoring is started. However, the supporting piles at the follow-up detection points JC26 ~ JC28 and the supporting piles at the corner of the BC section are all being poured. Limited by the red-line enclosure of the site, the pump truck can only be parked within the excavation area of the foundation pit. The sudden increase of additional load will bring some disturbance to the supporting pile, which leads to the positive horizontal lateral values of the monitoring points JC23 ~ JC25 in the construction process of adjacent supporting piles.

After the 22nd period, the JC23~JC28 monitoring points' horizontal displacement change rate suddenly went up. The amount of horizontal displacement change was also large, and the front piles' horizontal displacement surge at JC23, JC25, and JC27 monitoring points was easier to see. Since the foundation pit will be constructed after the 22nd period, the foundation floor and some building bodies will also begin to be constructed. The additional load will increase in a short time in the material transport lane, 5 meters away from the edge of the foundation pit, and the increased additional load will be further transmitted to the front row piles of the pile supporting structure. Furthermore, the additional load generated by the puddles outside the monitoring points JC23, JC25, and JC27 will also be transferred to the front piles through the soil. The front-row piles will bear greater active earth pressure, which will lead to a sudden increase in their horizontal displacement. At this time, the horizontal displacement curve of the previous row of piles will pass through the horizontal displacement curve of other monitoring points and drop rapidly. The spatial variability of the soil layer and the difference in the soil layer that the front row piles pass through will also cause the horizontal displacement values of the front piles to be different.

Analysis of Numerical Simulation Results

Analysis of Cumulative Horizontal Displacement

The front-row pile with the back-pull pile, the front-row pile without the back-pull pile, and the back-pull pile aggregately have "upward convex" cumulative horizontal displacement curves, as seen in Figure (6). The top of the supporting pile is where the pile body's maximum displacement is found, and from there, the displacement value progressively drops along the pile's depth direction until it almost reaches zero (Gu, 2014; Zhou et al., 2016).

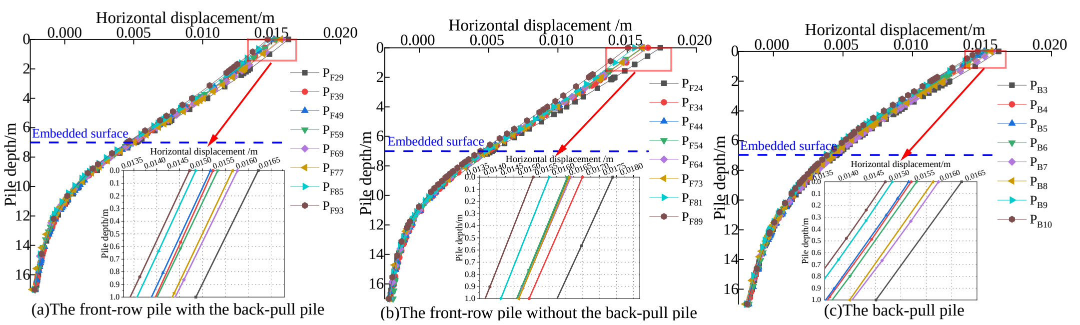

Figure (6): The cumulative horizontal displacement curve of monitoring point

The maximum horizontal displacement value of similar supporting piles varies slightly due to the type and thickness of the soil layers that they pass through. Compared with the maximum horizontal displacement of the three types of supporting piles, the maximum horizontal displacement of the top of the front-row pile with the back-pull pile is slightly greater than that of the top of the pile with the back-pull pile, and the maximum horizontal displacement of the front-row pile with the back-pull pile and the back-pull pile is smaller than that of the front-row pile without the back-pull pile. Analysis of the reasons shows that the front-row pile without the back-pull pile is essentially a single-row pile, and its stability and service performance are far less than the frame structure composed of the front-row pile and the back-pull pile. Therefore, the displacement of the front-row pile without the back-pull pile is slightly larger than those of other types of supporting piles in the same foundation pit support structure (Zheng et al., 2021; Yi et al., 2022).

Analysis of Cumulative Pile Bending Moment

The front-row pile's bending moment curves are combined into an "inverted S" shape, as seen in Figure (7). Specifically, there are two reverse bending points; namely, the maximum positive bending moment point and the maximum negative bending moment point. The bending moment curve of the back-pull pile body presents a "bow" shape and only contains one reverse bending point, which is the maximum negative bending moment point, and the maximum positive bending moment point is located at the top of the pile, which is similar to the back-row pile of the double-row pile support structure.

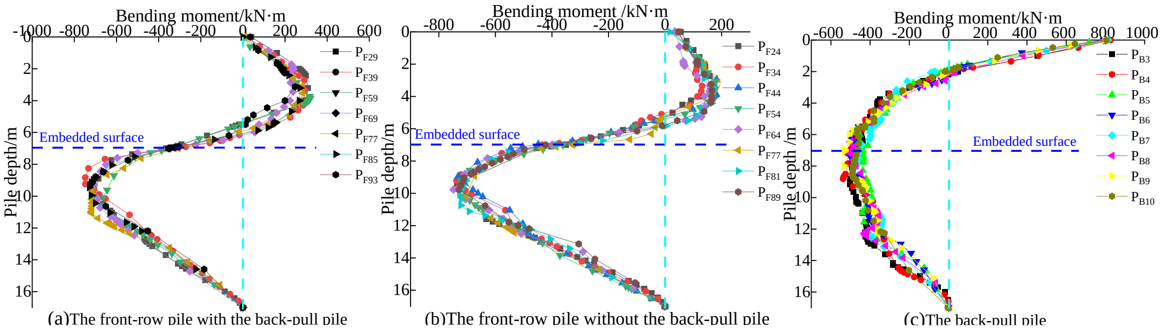

Figure (7): Bending moment curve of the piles

When the maximum positive bending moment values of the three different types of supporting piles are compared, as in Figure (8), it is evident that the front-row pile's maximum positive bending moment value is significantly smaller than the back-pull pile's. The mean value of the maximum positive bending moment of the back-pull pile is 2.78 times that of the front-row pile with the back-pull pile and 4.66 times that of the front-row pile without the back-pull pile. The positive bending moment value of the back-pull pile is larger, because it is subjected to the dynamic earth pressure and static earth pressure behind the pile and the pulling force from the three connecting beams. Among the front-row piles, the maximum positive bending moment of the front-row pile with the back-pull pile is 1.68 times the maximum positive bending moment of the front-row pile without the back-pull pile, and the maximum negative bending moment of the front-row pile without the back-pull pile is 1.03 times the maximum negative bending moment of the front-row pile with the back-pull pile.

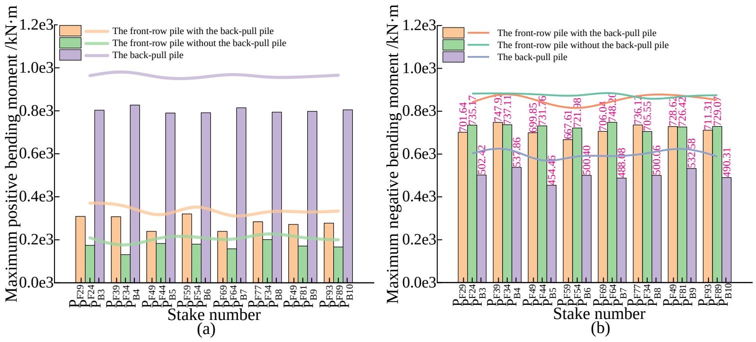

Figure (8): Bending moment comparison diagram

Comprehensive comparison can show that the front-row piles without the back-pull pile show the characteristics of large horizontal displacement, a small positive bending moment, and a large negative bending moment. The horizontal displacement of the front-row pile without the back-pull pile is large, and the soil behind piles can fully release its shear strength, so the active earth pressure decreases and the positive bending moment is small. However, the pile body of the front-row pile without the back-pull pile will continue to squeeze the soil in the passive area while moving to the inside of the pit, and the passive soil pressure will increase accordingly, so the negative bending moment is larger. After adding the back-pull pile to the back of a single-row pile, the back-pull pile, connecting beam, and front-row pile with the back-pull pile can form a more stable "portal" frame structure, which can jointly resist the deformation of active soil, inhibit the release of stress, and control the displacement of the front pile. In terms of the distribution of positive and negative bending moments of pile body, the front-row pile with back-pull pile has a more reasonable distribution of positive and negative bending moments of pile body than the front-row pile without back-pull pile, and the zero bending moment point is closer to the embedded surface. It can be seen that the back-pull pile can improve the uneven distribution of bending moments in the single-row pile.

DISCUSSION

It can be seen from Figure (9 (a)) that the displacement change trend of the monitoring results and the numerical simulation results is consistent, both of which can reflect the "wavy characteristics" of the crown beam, but the values of the same monitoring point are still different. Since idealized numerical modeling cannot reproduce extremely complex practical projects, the disturbance of soil samples during the acquisition of soil parameters will cause a difference between the obtained parameters and the parameters of undisturbed soil, which further causes a difference between the monitored values and the simulated values.

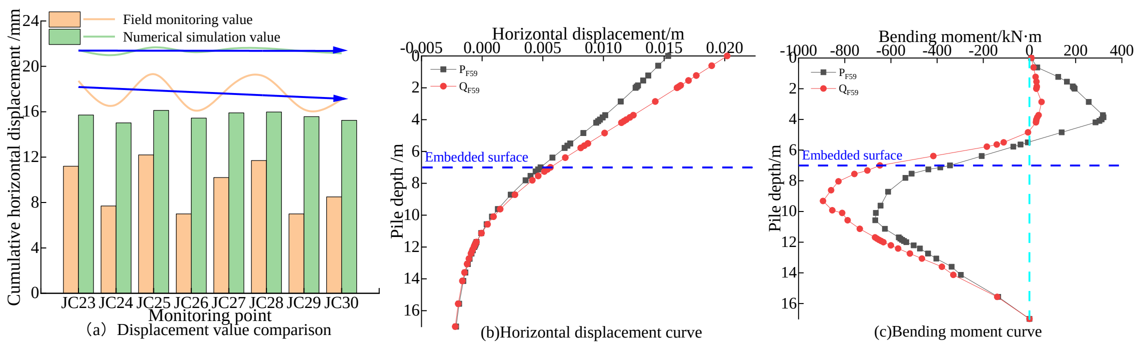

Figure (9): Displacement comparison and comparison of pile P_{F59} and pile Q_{F59}

The single-row pile and the front-row pile with the back-pull pile are compared and analyzed. As shown in Figure (9 (b)), the displacement curve of the front-row pile with the back-pull pile P_{F59} is similar to that of the single-row pile Q_{F59}, both showing a “convex” shape. However, the bending degree of the horizontal displacement curve of the two is obviously different. The horizontal displacement of the pile P_{F59} is smaller than that of the pile Q_{F59}, and the difference is about 4.87 mm. Above the embedded surface of the pile, the horizontal displacement curve swing of pile P_{F59} is smaller than that of pile Q_{F59}.As shown in Figure (9(c)), the bending moment curve of single-row piles is similar to that of front-row piles with back-pull piles and also presents an “inverted S” shape. However, the bending moment distribution of the single-row pile body is also very uneven, and the negative bending moment accounts for a larger proportion in the distribution of positive and negative bending moments along the depth direction of the pile. The average value of the maximum negative bending moment of each single-row pile is 14.54 times the average positive bending moment, and the difference is large. The back-pull pile makes the zero bending moment point of the single-row pile rise by nearly 0.7 m, while the positive bending moment value increases by 412.51 %, and the negative bending moment value decreases by 25.32 %, which makes the bending moment distribution of the single-row pile more reasonable; that is, the "back-pull pile effect".

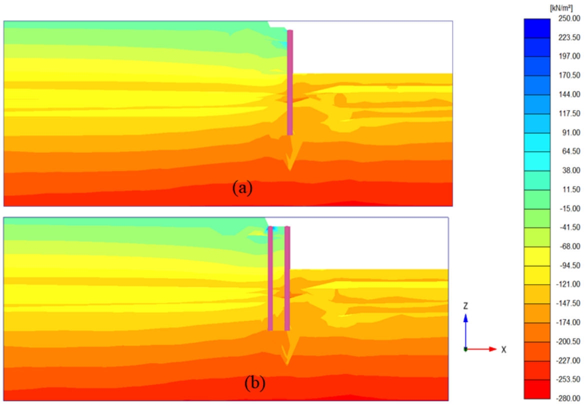

Figure (10): Cartesian cloud map of the effective shear stress of soil in a foundation pit: (a) The vertical section of pile Q_{F59}; (b) The vertical section of pile P_{F59}

As shown in Figure (10), the Descartes effective shear stress of soil behind the single-row pile Q_{F59} is significantly greater than that behind the front-row pile with the back-pull pile P_{F59}, and the maximum Cartesian effective stress of soil behind both piles occurs around 2.8m and 3.8m in the direction of the pile body, respectively. However, the maximum value of Descartes effective stress of soil around the pile is near the top of the pile. The above Descartes effective shear stress distribution characteristics correspond to the horizontal displacement of the supporting pile and the change law of the bending moment of the pile body: the Descartes effective shear stress of the soil in the active area behind the single row pile is large, the Descartes effective compressive stress is small, and the positive bending value is small; the Descartes effective shear stress of the soil in the active zone behind the front-row pile with the back-pull pile is small, the Descartes effective compressive stress is large, and the positive bending value is large.

The horizontal displacement of the single-row pile is large, and the soil behind the pile can fully release its shear strength to resist the relative dislocation between the soil and the soil. In other words, the soil behind the pile uses its shear strength to counteract the shear stress that the lateral confinement relaxation has caused. The soil behind the single-row pile is in the ultimate stress state when the lateral confinement is relaxed. Therefore, the Descartes effective pressure borne by the single-row pile is smaller than that of the front-row pile with the back-pulling pile, as shown in Figure 11(a) and (b). The horizontal displacement of the single-row pile is large, and the squeezing degree of the soil in the passive zone in front of the pile is also large, and the Descartes effective compressive stress of the soil in the passive zone increases accordingly. Therefore, the Descartes effective compressive stress of the soil in the passive zone in front of the single-row pile is greater than the Descartes effective compressive stress of the soil in the passive zone in front of the back-pull pile, as shown in Figure 11(c) and (d). It can be seen that the "back-pull pile effect' can change the bending moment distribution of the single-row piles by changing the stress state of the soil and can also reduce the horizontal displacement of the front-row pile, even if the PPSS has better lateral displacement resistance.

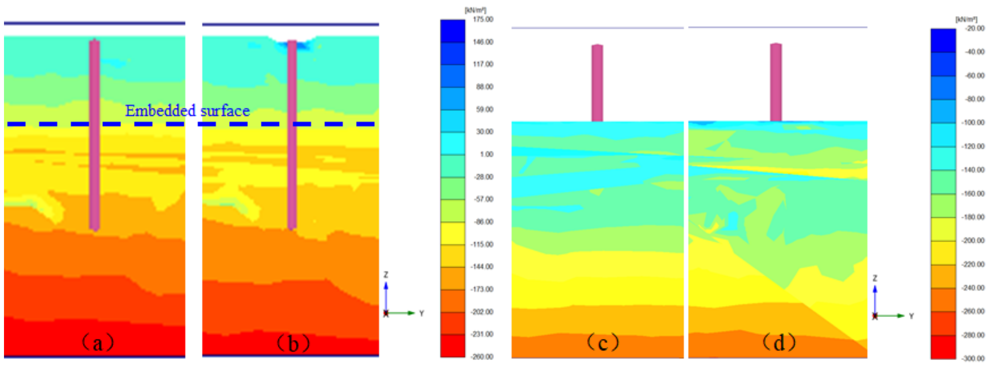

Figure (11): Cartesian cloud map of the effective compressive stress of soil in the cross-section of the foundation pit: (a) Cross-section of soil behind pile Q_{F59}; (b) Cross-section of soil behind pile P_{F59}; (c) Cross-section of soil in front of pile Q_{F59}; (d) Cross-section of soil in front of pile P_{F59}

In summary, the number of back-pull piles, which is only 10.7% of the number of front-row piles, can greatly reduce the horizontal displacement of the front-row pile and can also improve the uneven distribution of positive and negative bending moments of the single-row piles. It can be seen that the back-pull pile plays a good supporting role in reducing the displacement of the front-row piles; that is, the PPSS has good safety and serviceability and can well control the lateral displacement of the foundation pit. The supporting effect of the three types of supporting piles can be more directly highlighted by adding the back-pull piles at the rear of the single-row piles: the back-pull piles mainly bear positive bending moments, and the front-row piles mainly bear negative bending moments. According to the distribution law of such a bending moment, the three types of supporting piles can be designed separately, so that the back-pull piles and the front-row piles have good safety and serviceability, and the supporting structure of the pulling piles can meet the requirements of "solving large height differences in small spaces" (Hu et al., 2021; Wang et al., 2022; Lan et al., 2023).

CONCLUSIONS

Based on the analysis of the results of this study, the following main conclusions are drawn:

(1) The deformation law of the PPSS is similar to that of the cantilever pile without internal support. The cumulative horizontal displacement curves of the three types of supporting piles show a "convex" shape. The bending-moment curves of the front-row pile are all in the shape of an "inverted S", and the whole shows the law of small in the upper and large in the lower. The bending-moment curves of the back-pull pile are all "bow"-shaped.

(2) In the process of studying the work principles of the back-pull pile, it was also found that the back-pull pile can highlight the supporting role of the three types of supporting piles more directly: the back-pull pile mainly bears positive bending moments, and the front-row pile mainly bears negative bending moments. According to the distribution law of bending moment, the three kinds of supporting piles can be designed separately to make the PPSS play its supporting role better.

(3) The "back-pull-pile effect" can improve the unbalanced distribution of positive and negative bending moments of single-row piles by changing the stress condition of the soil and can also effectively reduce the displacement of single-row front piles. In other words, the pull-pile supporting structure has good safety and serviceability and can well control the lateral displacement of the foundation pit.

Funding

This research was funded by the Natural Science Foundation of Shandong Province, China (ZR2021MD011).

Acknowledgements

The authors gratefully acknowledge the financial support from the Natural Science Foundation of Shandong Province (ZR2021MD011), and School of Civil Engineering and Geomatics, Shandong University of Technology. Thanks are also due to Chengdu Institute of Survey and Investigations, for providing project information, as well as Tianjinchengjian University, School of Materials Science and Engineering, for providing software support.

REFERENCES

Gan, F., Zheng, G., Cao, T., Zhou, H.Z., Jiang, Z.H., Li, M.X., Bi, J., and Li, Y.L. (2023). "Experimental study on retaining structure of alternating combination of vertical and inclined steel-pipe piles". Yanshilixue Yu Gongcheng Xuebao/Chinese Journal of Rock Mechanics and Engineering, 42 (5), 1175-1187.

Gu, L. (2014). "Finite element analysis and investigation of double-row piles supporting". Advanced Materials Research, 779-785, 838-841.

Guo, J.Z., Li, X.H, Cheng, X.S, Pei, H.T., Wang, Y.P., and Zheng, G. (2023). "Study on design and calculation method for vertical and inward-inclined pile retaining structure of excavation". Tumu Gongcheng Xuebao/China Civil Engineering Journal, 56 (8), 153-163.

Hu, Y., Guo, T.D., Long, W.X., Jiang. B., and He, J. (2021). “Research on deformation characteristics and internal forces of double-row circular piles based on BOTDA distributed optical fiber sensing technology”. Journal of Xi'an University of Architecture and Technology (Natural Science Edition). 53 (05), 692-699.

Jiang Y.N., Chen R.Z.,Shao S.L., and Xu, C.C. (2022). “The behavior and optimization analysis of double-row piles in different forms”. Jordan Journal of Civil Engineering, 16 (3), 365-380.

Lan, B.P., Wang, Y.P, and Wang, W.G. (2023). “Review of the double-row pile supporting structure and its force and deformation characteristics”. Applied Science-Basel, 13 (13), 7715.

Liu, C., Ma, L.Y., Zheng, G., Yan, C.D., and Yang, Y.H. (2022). “Field measurement and mechanism of inclined and vertical piles in foundation pits”. Yantu Gongcheng Xuebao/Chinese Journal of Geotechnical Engineering, 44 (5), 827-835.

Mo, P.Q., Liu, Y., Huang, Z.F., Teng, H.B., Chen, B., and Tao, X.L. (2022). “Compatibility of deformation and spatial effects for retaining pile, crown beam and braces under complex retaining conditions of deep foundation pit”. Rock and Soil Mechanics, 43 (09), 2592-2601.

Qian, G., and Guo, Y. (2011). “Numerical simulation of working performance for retaining structure with double-row piles”. 2nd International Conference on Mechanic Automation and Control Engineering. MACE 2011-Proceedings. IEEE Computer Society. New York, USA.

Sun, T., Liu, J.Y., and Liu, Y. (2012). “Optimal row distance of retaining structure with double-row piles”. Chinese Journal of Geotechnical Engineering, 34 (S1), 616-620.

Wang, G., Dong, C.G., Fang, Z., Chang, S., and Singh, J. (2022). “Parameter study on double-row pile in the combined high retaining structure”. Geotechnical and Geological Engineering, 40 (10), 5233-5248.

Wang, L, Dai, Y., and Liu, G. (2024). “Mechanical difference analysis of single-row and double-row side piles in stations by PBA method based on model test”. Jordan Journal of Civil Engineering, 18 (1), 146-159.

Yang, S.J., Ma, J.X., Wang, Y.H., and Sun, S.X. (2020). “Experimental study on mechanical behavior of micro-tube piles in deep soil rock foundation pits”. Science Technology and Engineering, 20 (30), 12540-12545.

Yang, Y.B., Chen, C.Y., Liu, C., Huang, L.T., Chen, W., and Lin, N.Y. (2023). “Performance of a deep excavation and the influence on adjacent piles: A case history in karst region covered by clay and sand”. Underground Space, 8, 45-60.

Ye, J.B., Wang, C.F., Huang, W.P., Zhang, J., and Zhou, X.Q. (2020). “Effect of inclination angle on the response of double-row retaining piles: Experimental and numerical investigation”. Tehnicki Vjesnik, 27 (4), 1150-1159.

Yi, F., Su, J., and Zheng, G. (2022). “Overturning progressive collapse mechanism and control methods of excavations retained by cantilever piles”. Engineering Failure Analysis, 140, 106591-106610.

Yu, F., Xie, Z.B., Duan, N., Liu, N.W., and Shan, H.F. (2019). “Performance of double-row piles retaining excavation beneath existing underground space”. International Journal of Physical Modeling in Geotechnics, 19 (04), 167-180.

Zhang, M.Y., Ma, J.X., Yang, S.J., Wang, Y.H., Bai, X.Y., and Sun, S.X. (2020). “Experimental study on bending moment of double-row steel-pipe piles in foundation excavation”. Advances in Civil Engineering, 19, 8882712.1-8882712.8.

Zheng, G., Yi, F., Huang, T.M., Cheng, X.S., and Yu, D.Y. (2021). “Mechanism of overturning progressive collapse of excavations retained by double-row piles induced by over-excavation”. Chinese Journal of Geotechnical Engineering, 43 (8), 1373-1381.

Zhou, J.P., Huang, X.F., Yuan, J., Zhang, J.L., and Wang, X.M. (2021). “Comparative study on the influence of pile length and diameter on bearing capacity and efficiency of root piles, straight-shaft piles and pedestal piles”. Arabian Journal for Science and Engineering, 46 (11), 104439-10456.

Zhou, Y.J., Liu, K.M., and Wang, F.N. (2021). “Research on the mechanical properties of new double-row pile supporting structure based on an in situ study”. Shock and Vibration, 2021.

Zhou, Y.J., Luo, L.G, and Zhang, L.X. (2022). “Review of the deformation mechanism and earth pressure research on the double-row pile support structure”. Frontiers in Earth Science, 10, 933840-933845.

Zhou, Y.J., Yao, A.J., Li, H.B., and Zheng, X. (2016). "Correction of earth pressure and analysis of deformation for double-row piles in foundation excavation in Changchun of China". Advances in Materials Science and Engineering, 2016, 9818160.

Zhu, Y.X., Qin, H.L., Zhang, X.P., Wei, D.S., Zhai, L., and Hu, L.X. (2024). "Innovative three-row pile support system of ultra-deep foundation pit and cooperative construction technology with basement for high-rise tower structures". Buildings, 14 (4), 1003.